BIOTITE ALTERATION IN DEEPLY WEATHERED GRANITE. I. MORPHOLOGICAL, MINERALOGICAL, AND CHEMICAL PROPERTIES

R. J. GILKES AND ANCHALEE SUDDHIPRAKARN[1]

Department of Soil Science and Plant Nutrition, University of Western Australia
Nedlands, Western Australia, Australia 6009

Abstract—Biotite in deeply weathered granitic rocks in southwestern Australia has altered to exfoliated grains composed of biotite, mixed-layer clay minerals, kaolinite, vermiculite, gibbsite, goethite, and hematite. Discrete vermiculite and vermiculite-dominant mixed-layer clay minerals are not major weathering products. Oxidation of octahedral iron in biotite is associated with ejection of octahedral cations, loss of interlayer K, and a contraction of the b-dimension of the biotite sheet. Si, Mg, Ca, Mn, K, and Na are lost from biotite during weathering, and Ti, Al, Ni, and Cr are retained. Fe and water have been added to the grains during weathering. Much Fe occurs as aggregates of microcrystalline, aluminum-rich goethite particles on flake surfaces and within etchpits, with smaller amounts occurring as hexagonal arrangements of lath-shaped crystals of goethite on flake surfaces.

Key Words—Biotite, Goethite, Mixed-layer mineral, SEM morphology, Vermiculite, Weathering.

INTRODUCTION

Biotite in soils is considered to be an important source of potassium and minor elements for plants, and a large number of workers have been prompted to investigate the morphological, mineralogical, and chemical features affecting the release of ions from biotite during synthetic weathering (see recent reviews by Reichenbach and Rich, 1975; Fanning and Keramidas, 1977). In laboratory experiments biotite alters to vermiculite or mixed-layer clay minerals, whereas the products of natural weathering may also be kaolinite, halloysite, illite, smectite, chlorite, and sesquioxides. In contrast to the abundant data on synthetic weathering products there is relatively little published information dealing with the nature of naturally weathered biotite grains.

This paper describes some morphological, mineralogical, and chemical properties of altered biotite grains from deeply weathered soil profiles on granitic rocks in southwestern Australia.

SAMPLING AND METHODS

Altered biotite grains were obtained from deeply weathered Archean granitic rocks (adamellites) exposed in a railway cutting at Jarrahdale, a bauxite mining center 45 km southeast of Perth, Western Australia. The typical lateritic soil profile at this locality is about 10 m deep and consists of the following horizons: sandy gravel and duricrust, ferruginous zone, mottled zone, pallid zone, saprolite, and parent rock. Detailed mapping and mineralogical examination of these soils have shown that the saprolite and pallid zone materials derived *in situ* from the underlying granitic rocks (Sadleir and Gilkes, 1976).

Five-kilogram samples were taken from various levels in the saprolite and pallid zones and from the parent materials at two adjacent sites (R, L profiles), and from a third site 200 m distant (B profile). Undisturbed subsamples were impregnated with Araldite F resin and thin sectioned for optical examination. Altered biotite grains (~1 mm) were separated from the bulk samples using a combination of gentle dispersion, sedimentation, sieving, magnetic and density fractionation, and hand-picking under a stereomicroscope. Some specimens were separated into grains that sank in bromoform (heavy) and those that floated (light).

The composition of altered biotite grains was determined by X-ray diffraction (XRD) using a Gandolfi single crystal camera (Gandolfi, 1967) with Fe-filtered cobalt radiation. XRD patterns of random powders were obtained using a Philips diffractometer with cobalt radiation. Accurate measurements of the spacing of the 060 reflection were obtained by automatic step-scanning over the 2θ range 70.5–71.7°. Counts were accumulated for 20 seconds at 0.02° intervals and peak positions located graphically. Basally oriented preparations of finely ground altered biotite on porous ceramic plates were analyzed by XRD after the various pretreatments mentioned below.

Bulk samples of grains from various horizons of each profile were finely ground, saturated with Ca, and dried at 105°C prior to chemical analysis. Minor amounts of quartz and other impurities were present in all samples. Fe, Al, Si, Ca, K, Mg, Ti, and Mn were determined by

---

[1] Permanent address: Department of Soil Science, Kasetsart University, Bangkok, Thailand.

349
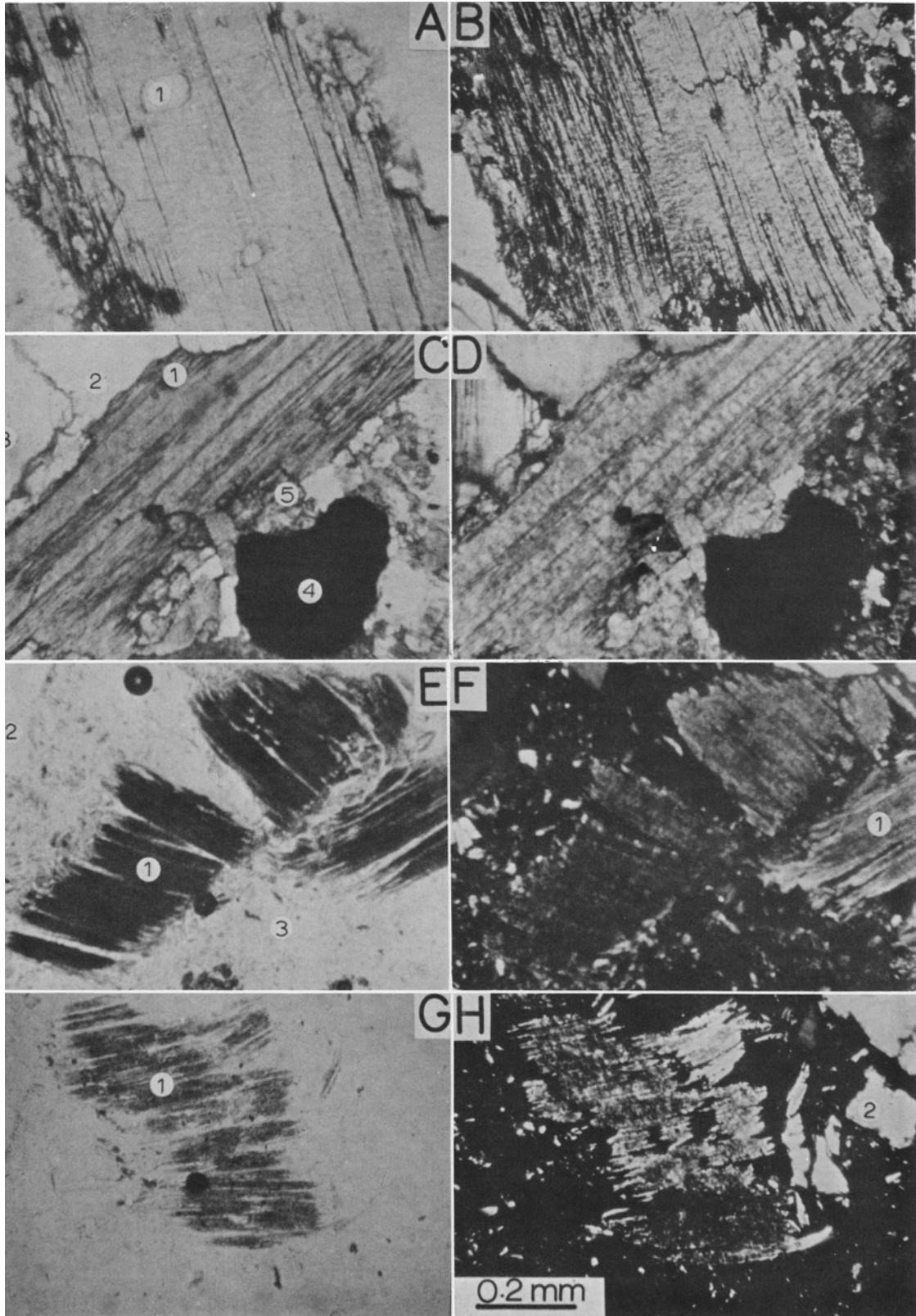
X-ray fluorescence spectrometry after fusion in a lithium borate–lanthanum oxide flux following the method of Norrish and Hutton (1969). Zn, Ni, Cr, and Na were determined by atomic absorption spectrophotometry after dissolution in mixed hydrofluoric and perchloric acids. Ferrous iron was determined by dichromate titration after dissolution of samples in mixed HCl and HF acids under a nitrogen atmosphere. Water content was determined by ignition of 900°C. The reliability of the analytical procedures was checked by analysis of standard mineral specimens.

Whole altered biotite grains were impregnated with epoxy resin and polished sections made either parallel or normal to the biotite cleavage for qualitative electron microprobe analysis using an ARL-SEMQ instrument.

Altered biotite grains were investigated by scanning electron microscopy (SEM) using a Philips PSEM 500 instrument. Specimens were mounted on aluminum stubs and coated with a 20-Å layer of gold in a vacuum evaporator. Biotite flakes were mounted for SEM examination both normal and parallel to the cleavage plane. Some flakes were cleaved with a needle along nonexfoliated planes; others were pulled apart with cellulose adhesive tape to expose fresh surfaces. Platinum-shadowed carbon replicas of cleaved surfaces were prepared to provide more detail of the morphology of fine-grained alteration products by transmission electron microscopy (TEM) using a Hitachi HU IIB instrument. Freshly exposed cleaved surfaces were also gently scraped with a scalpel blade to remove surface materials for TEM examination and selected area electron diffraction (SAD).

RESULTS AND DISCUSSION

Morphological properties

A representative series of optical micrographs illustrating the progressive alteration of biotite grains is shown in Figure 1. Fresh biotite in the parent materials exhibited high birefringence and pleochroism which decreased with increasing alteration. Within a single horizon in the saprolite and pallid zones, grains at various stages of alteration occurred. The most altered grains occurred closer to the surface. Biotite flakes in contact with quartz were less altered than those in contact with feldspar. At an early stage of alteration exfoliation and infilling with alteration products occurred.
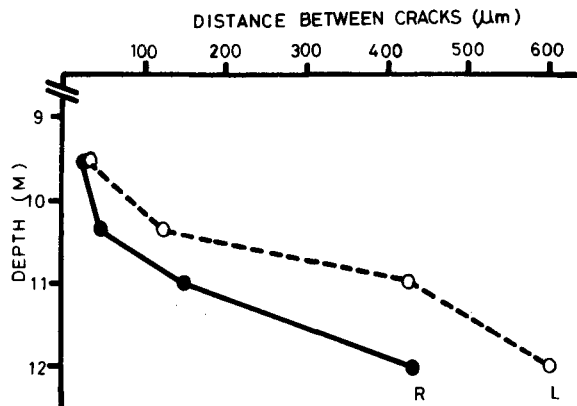
Figure 2. The distance between cracks in exfoliated altered biotite in saprolite and pallid zones of R and L profiles as a function of depth in the profile.

Measurements of the average distance between opened cleavages are shown in Figure 2 and substantiate the qualitative impression given by the micrographs in Figure 1 by demonstrating a systematic increase in exfoliation towards the surface.

Altered biotite flakes from the saprolite showed SEM features consistent with those observed in thin sections. Extensive exfoliation has occurred, and fine-grained alteration products coated grain surfaces (Figure 3A). In the fragile, highly exfoliated pseudomorphs occurring in the pallid zone, deposits of fine-grained secondary minerals were noted between widely exfoliated layers (Figure 3B). The basal surfaces of these flakes are highly etched, and extensive regions of fine-grained alteration products are present on the surfaces (Figure 3C).

The smooth surfaces exposed by the cellulose adhesive tape technique showed rolling-up of micaceous materials and were heavily but discontinuously coated with fine-grained alteration products. In some regions small ($\sim$0.1 $\times$ 0.01 μm), lath-shaped crystals were arranged in hexagonally oriented patterns. These alteration products were commonly present in concavities or etch pits within the flat micaceous surfaces which were bounded by 20- to 200-Å deep steps (Figure 4). Electron and X-ray diffraction patterns showed that much of the fine-grained material and the hexagonally oriented laths consisted of goethite (Gilkes and Suddhiprakarn, 1979).

←

Figure 1. Optical micrographs of thin sections of saprolite and pallid zone materials showing various stages of alteration of biotite grains. (A) Saprolite, a highly birefringent biotite grain is partially exfoliated (1). (B) Saprolite, partially exfoliated, birefringent biotite grain. (C, D) Saprolite, a weakly birefringent biotite grain (1) exhibiting major exfoliation with zones of relatively unaltered biotite between opened cleavages. Where flakes are in contact with quartz (2) they are generally less altered than where they are in contact with feldspar (3) or epidote (5). The opaque mineral is probably magnetite (4). (E, F, G, H) Pallid zone, very highly altered biotite (1) which has been mainly replaced by secondary minerals showing major exfoliation and infilling between fragments. Undulose quartz (2) and partly altered feldspar (3) are present. (A, C, E, G, plane polarized light; B, D, F, H, crossed polarizers.)
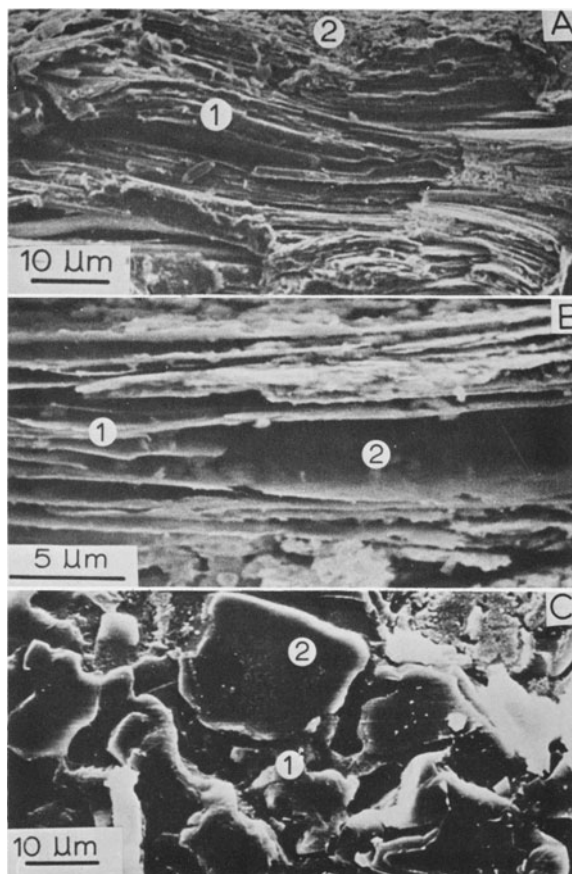
Figure 3. Scanning electron micrographs of altered biotite grains. (A) Saprolite, the edge of an exfoliated grain (1) coated with fine-grained alteration products (2). (B) Pallid zone, the edge of a highly exfoliated grain (1) with fine-grained alteration products present between layers (2). (C) Pallid zone, the basal surface of an exfoliated grain with a highly etched surface (1) coated with fine-grained alteration products (2).
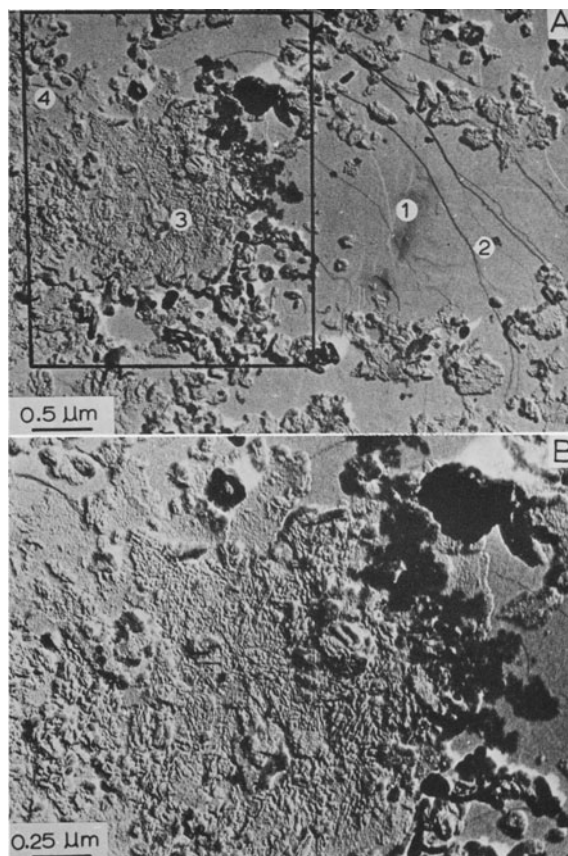

Figure 4. Replica electron micrographs of a basal surface of a cleaved altered biotite grain from the pallid zone. (A) Shallow etchpits in the smooth micaceous surface (1) are bounded by 20- to 200-Å deep steps (2). Very small lath-shaped (3) and platy crystals (4) are present on the surface. (B) A photographic enlargement of the rectangular area in A. The lath-shaped and platy crystals on the micaceous surface are more clearly seen but their morphology remains poorly resolved by this technique.

Basal surfaces exposed by cleaving with a needle corresponded to nonexfoliated or more difficult cleavages and showed more extensive smooth micaceous areas with little fine-grained material.

The detailed morphology of the fine-grained alteration products was investigated by TEM on scrapings from basal surfaces of exfoliated flakes from the pallid zone. A great variety of materials was observed of which the following types were most abundant. Micaceous fragments were very common (Figure 5A), their SAD patterns commonly showed superimposed hk0 nets with d(060) = 1.53 Å indicating that they consist of several fragments of a trioctahedral layer-silicate at different orientations within the (001) plane (Figure 5B). The moiré patterns observed in the images of these flakes are consistent with this interpretation (Suito and Nakahira, 1971). Many micaceous fragments contain or are coated with aggregates of very fine-grained (0.02

μm) alteration products which may be kaolinite or goethite (Figure 5C). Hexagonal orientations of lathlike goethite are present on mica (Figure 5D) or as discrete particles (Figure 5E).

Eswaran and co-workers (Eswaran and Heng, 1976; Eswaran and Bin, 1978) described pseudomorphs of biotite from tropical soils which consisted of mixtures of mixed-layer minerals, tubular halloysite, kaolinite, and goethite. In the present work, however, tubular halloysite was not found to be a weathering product of biotite despite its presence as the major weathering product of associated feldspars. Also, Eswaran and co-workers found goethite as intersecting, 1-μm size lamellae at the edges of flakes in horizons of iron oxide accumulation. They suggested that this coating inhibited further alteration of the enclosed mixed-layer mineral. It was not present on iron-deficient pseudomorphs
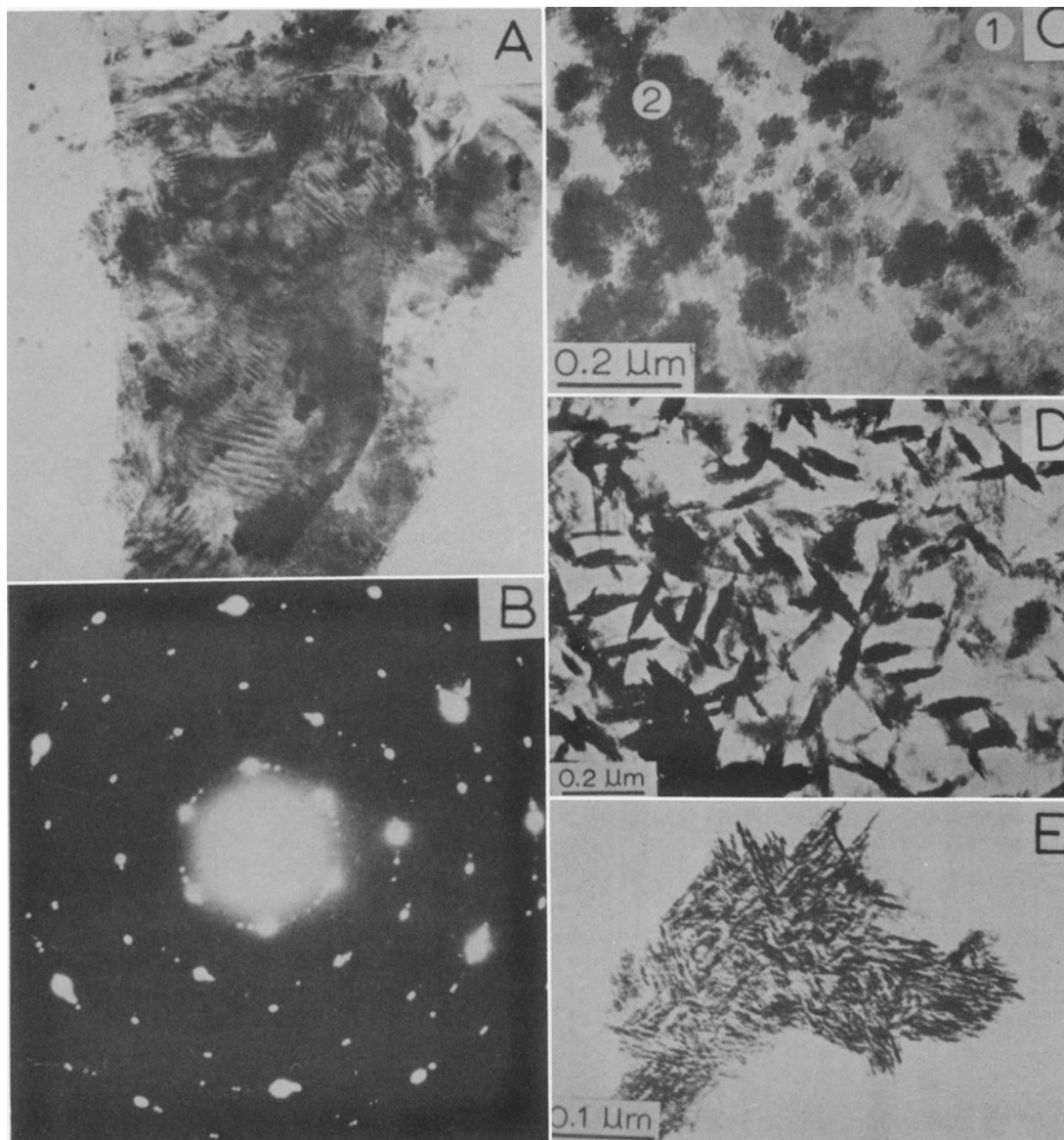
Figure 5. Transmission electron micrographs of materials scraped from cleaved surfaces of altered biotite grains from the pallid zone. (A) Micaceous material exhibiting moiré patterns. (B) SAD pattern of the material shown in A. (C) Micaceous material (1) with aggregates of fine-grained alteration product (2). (D) Micaceous material covered with hexagonally arranged aggregates of lath-shaped crystals. (E) A discrete hexagonally arranged aggregate of lath-shaped crystals.

in the pallid zone. In the present work, goethite was found as aggregates of microcrystalline material on the surface of flakes and within open cleavages, with lesser amounts as laths arranged in hexagonal orientations. Jackson *et al.* (1973) also found fine-grained hydrous oxide crusts on intermittent cleavage surfaces in naturally weathered micaceous vermiculite. The crusts resembled the cleaved surfaces associated with early stages of biotite alteration in Jarrahdale specimens. Microcrystalline iron oxides and clusters of fragile tubes (halloysite?) were observed on cleaved surfaces

of weathered biotites from Scottish soils (Farmer *et al.*, 1971). These authors observed hexagonally arranged laths of β-FeOOH (akaganéite) on cleaved surfaces of vermiculites oxidized in bromine water; however, β-FeOOH does not occur in soils (Schwertmann and Taylor, 1977), and the hexagonally arranged crystals found in the present work are goethite.

Mineralogical properties

The relative bulk mineralogy of altered biotite flakes was estimated semiquantitatively by XRD (Figure 6).
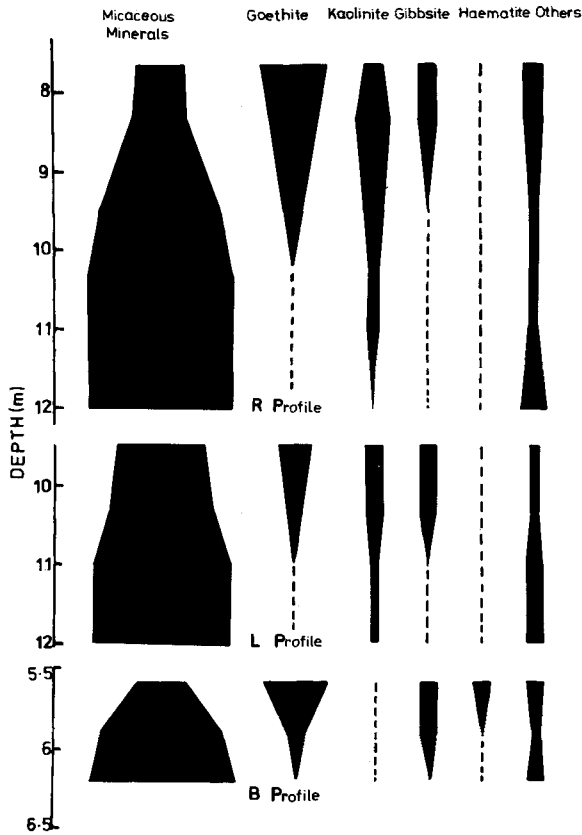
Figure 6.   Depth functions showing relative semiquantitative mineralogical composition of altered biotite grains from R, L, B deeply weathered profiles at Jarrahdale, southwestern Australia.
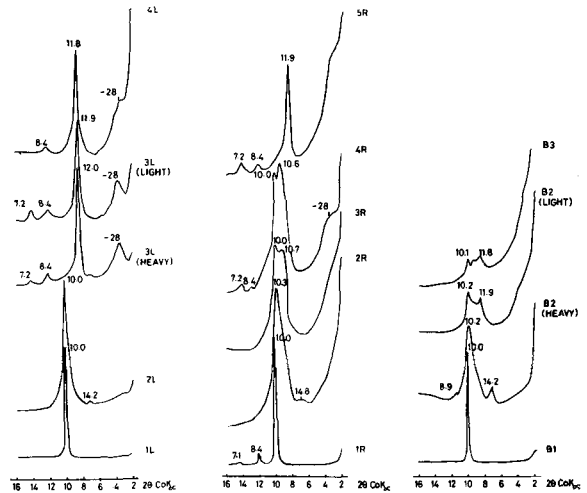

Figure 7.   Smoothed XRD patterns of basally oriented layer-silicate minerals present in altered biotite grains from the three Jarrahdale deeply weathered profiles. Spacings are in Å.

Small amounts of quartz, feldspar, and hornblende occur as inclusions in biotite grains. Biotite, vermiculite, and various mixed-layer clay minerals with different proportions of biotite and vermiculite are major constituents of altered biotite grains from every horizon. Goethite, kaolinite, and gibbsite are also present in R and L profiles; whereas gibbsite, goethite, and hematite are present in samples from B profile. The d spacings of the goethite indicate that 15–20 mole % AlOOH is present in solid solution in this mineral (Norrish and Taylor, 1961).

XRD patterns between 2 and 16° 2θ of basally oriented preparations of altered biotites are shown in Figure 7. These specimens had not been treated with a salt solution to replace the exchangeable cations since this pretreatment causes biotite to exchange some structural K with consequent modification of the XRD pattern. Little difference between the XRD patterns of light and heavy fractions was noted. Unaltered biotite is present in some specimens in association with mixed-layer clay minerals and probably represents both unaltered biotite grains and biotite cores of weathered grains. The sharp 10-Å reflection of biotite broadened and was systematically displaced towards higher spacings with increasing alteration. A poorly ordered hydrobiotite-like phase with reflections at approximately 28, 12, and 8.4 Å is present in the altered biotite grains. Similar poorly ordered structures can be reproduced in the laboratory by partial oxidation of structural iron in biotite and exchange of K by hydrated cations in some alternate interlayer (Gilkes, 1973; Norrish, 1973).

The proportion of biotite layers in the mixed-layer phases was estimated from the basal spacings on the assumption that the minerals are composed only of 10-Å biotite and 14-Å vermiculite layers (Ruiz-Amil *et al.*, 1967; Gilkes, 1973). For each specimen, biotite layers in excess of those needed for perfectly regular alternation of layers are present, i.e., using the nomenclature of Ruiz-Amil *et al.* (1967), the proportion of 10-Å layers, p(10 Å), was more than 0.5. It seems probable that once the hydrobiotite-like mineral formed, subsequent alteration mainly produced kaolinite, goethite, gibbsite, and hematite, rather than discrete grains of vermiculite or a mixed-layer clay mineral with excess vermiculite layers [p(10 Å) < 0.5]. Laboratory weathering experiments have shown that mixed-layer clay minerals with p(10 Å) < 0.5 do not usually form in K-depleted oxybiotites; instead, a vermiculite fringe [p(10 Å) = 0.0] develops around grains (Gilkes, 1973). Similarly, K-fixation by vermiculites only produces mixed-layer clay minerals with p(10 Å) > 0.5 (Rhoades and Coleman, 1967; Sawhney, 1967).

Vermiculite is present only as a minor constituent in altered biotite specimens, although it readily develops when these specimens are treated with potassium-free 1 M $MgCl_2$ (Figure 8C). Oxidation probably preceded

Figure 8. Smoothed XRD patterns of basally oriented layer-silicate minerals present in altered biotite grains from a Jarrahdale deeply weathered profile after various treatments. (A) Air dried after K saturation. (B) Heated at 400°C after K saturation (C) Air dried after Mg saturation. Spacings are indicated in Å.

Figure 9. Depth functions of the spacing of the 060 reflection of micaceous layers in altered biotite grains from the Jarrahdale deeply weathered profiles.

or accompanied K-exchange from biotite in these profiles, while potassium levels in ground waters were too high to enable the development of much discrete vermiculite or vermiculite-dominant mixed-layer clay mineral from the oxidized biotite. The hydrobiotite-like mineral subsequently altered to kaolinite, goethite, gibbsite, and hematite rather than to vermiculite. Treatment of altered biotite with 1 M KCl solution altered the XRD pattern but failed to fully collapse the vermiculite layers to 10 Å (Figure 8A). Diffraction patterns of the K-saturated specimens show a progressive increase in the abundance of vermiculite in the mixed-layer phase and an increasing proportion of kaolinite towards the surface of the soil. Clearly, most vermiculite layers did not collapse on K-saturation.

The morphological data show that fine-grained weathering products are present in scattered etchpits or concavities in mica surfaces, with the exception of exfoliated surfaces which are more highly etched and commonly thickly coated. The XRD patterns of K-saturated specimens which were heated to 400°C are consistent with this morphology since the mixed-layer minerals collapsed to give broadened 10-Å reflections (Figure 8B) indicating the presence of coherently diffracting packets of biotite layers that are smaller than those present in fresh biotite. Even in the highly altered biotite, most interlayers are not occupied by goethite or other weathering products, although some layers contain such deposits and therefore do not collapse to

a 10-Å spacing. Thus, the average size of coherently diffracting biotite zones decreased substantially on weathering resulting in broadened 10-Å reflections (Klug and Alexander, 1974). The very highly altered biotite from specimen 5R displayed a greatly broadened basal reflection at 10.2 Å after this treatment.

The position of the weak 060 reflection of residual altered biotite was estimated by drawing tangents to curves obtained by automatic step-scanning since maxima and centroid positions of the reflections could not be accurately determined due to their broad, flat-topped shape. In a few cases insufficient material or interference by a 1.54-Å quartz reflection prevented direct measurement. The 060 spacing decreases systematically towards the surface of each of the three profiles (Figure 9). Several authors have indicated that the b-dimension of micaceous minerals is related to chemical composition (Brindley and MacEwan, 1953; Radoslovich, 1963, 1975). A reduction in the content of K and octahedrally coordinated cations and an oxidation of Fe^{2+} result in a decrease in b-dimension. Under natural weathering conditions, changes in the nature of octahedral cations in biotite are usually associated with replacement of K by hydrated cations. Leonard and Weed (1970) showed by laboratory weathering experiments that the b-dimension of trioctahedral micas increases slightly on K-exchange. Artificial weathering studies of biotite involving both K-exchange and sub-
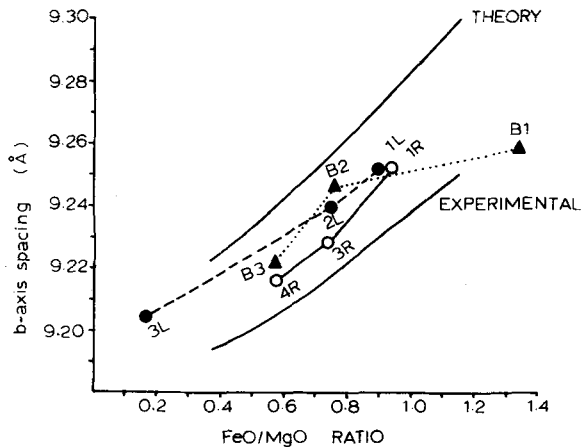
Figure 10. Changes in the FeO/MgO ratio and b-dimension of micaceous layers in altered biotite grains from the Jarrahdale deeply weathered profiles. The theoretical curve was calculated from the relationship derived by Brindley and MacEwan (1953) and the experimental curve is for artificially weathered biotite investigated by Gilkes *et al.* (1972).

stantial modification of the octahedral layer (Farmer *et al.*, 1971, Gilkes *et al.*, 1972) have shown a marked decrease in the b-dimension, in agreement with the results reported here.

The chemical composition of the residual micaceous layers in these specimens could not be determined due to the presence of kaolinite, gibbsite, goethite, and hematite. Neither Fe^{2+} nor Mg is likely to be a significant constituent of these alteration products; thus, the ratio of these elements in the altered biotite represents the ratio in the residual micaceous layers. The plot of Fe^{2+}/Mg vs. d(060) in Figure 10 shows a trend similar to the trends predicted by the theoretical formula of Brindley and MacEwan (1953) and the experimental results of Gilkes *et al.* (1972). Exact agreement would not be expected in either case. The theoretical formula requires a knowledge of the total chemical composition of the residual micaceous layers which cannot be determined. The chemical composition of the biotite used by Gilkes *et al.* (1972) differs from that of the biotite in the Jarrahdale profiles so that different b-dimensions would be anticipated. However, the similar trends support the concept that the b-dimension of residual mica layers reflects changes occurring in the nature of the octahedral cations due to oxidation of Fe^{2+} and ejection of octahedral cations.

Chemical properties

Fresh biotite in the parent granitic rock (adamellite) has the following structural formula based on 44 charge units per unit cell: $(Si_{5.66}Al_{2.34})(Ti_{0.17}Al_{0.29}Fe_{0.95}^{3+}Fe_{1.35}^{2+}Mn_{0.05}^{2+}Zn_{0.01}Mg_{2.66})O_{20}(OH)_4M_{1.79}^+$. The interlayer cation is denoted as M^+ since some K and Na were replaced during Ca-saturation.
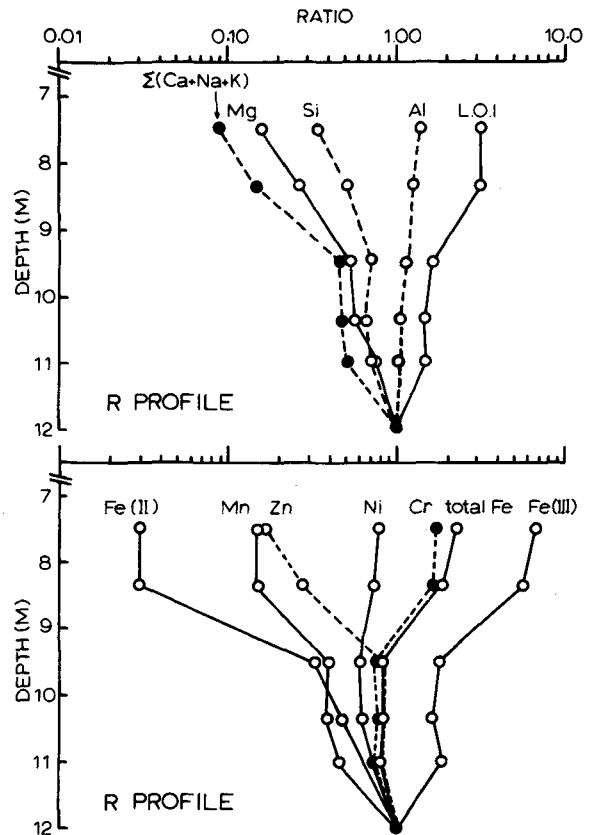

Figure 11. Depth functions showing the trends in chemical composition of altered biotite grains from R deeply weathered profile at Jarrahdale, southwestern Australia. The values are relative to the concentration of Ti and the ratios have been adjusted to unity for the parent biotite.

The incorporation of structural hydroxyl and water into secondary minerals during alteration resulted in dilution of all elements in the altered biotite grains. Furthermore, the ratio of residual elements was effectively increased by losses of the mobile elements K, Mg, etc. Consequently, absolute losses and gains of elements from weathering biotite grains can only be estimated by use of a reference element that is uniformly distributed in the original phase and wholly residual (immobile). Various elements, including Ti, Zr, and Al, have been used for this purpose in pedological studies. Relative changes in the chemical composition of altered biotite grains are shown in Figures 11 and 12 where Ti has been used as the wholly residual element. The Ti concentration is almost constant for altered grains from each profile so that the observed trends in chemical composition do not depend on the choice of reference. Titanium was originally present mainly in octahedral sites in biotite and as rare inclusions of rutile. Titanium probably remains in residual micaceous layers and as small crystals of anatase. Zirconium cannot be used as the
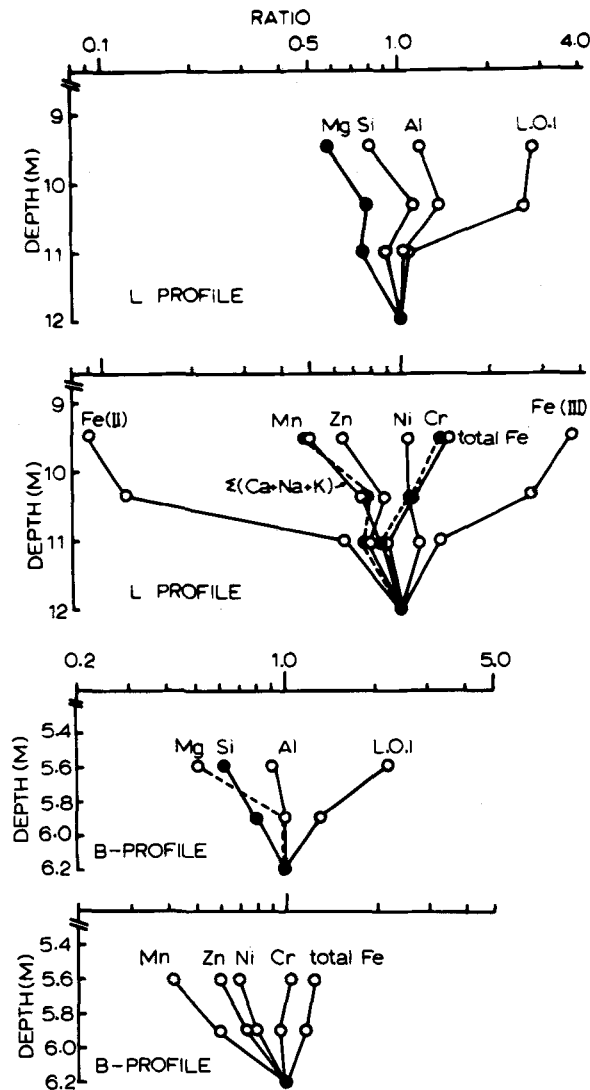
Figure 12. Depth functions showing the trends in chemical composition of altered biotite grains from L and B deeply weathered profiles at Jarrahdale, southwestern Australia. The values are relative to the concentration of Ti and the ratios have been adjusted to unity for the parent biotite.
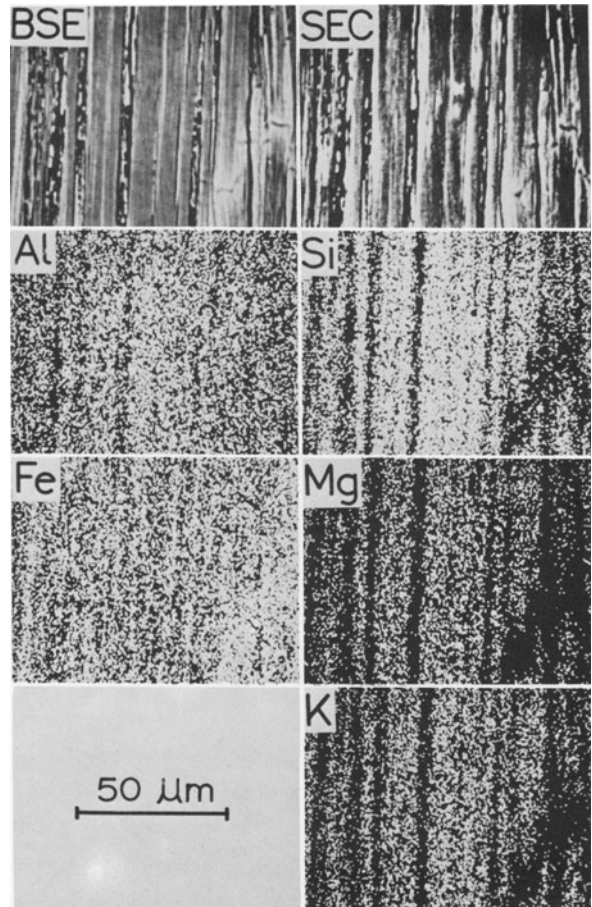

Figure 13. Electron-microprobe X-ray images showing the heterogenous distribution of Al, Fe, K, Mg, and Si in an altered biotite flake sectioned perpendicular to the cleavage. BSE—Back-scattered electron image; SEC—Secondary electron image.

reference element as it occurs mainly as zircon inclusions which are not uniformly distributed in biotite grains.

The behavior of major elements during weathering is generally consistent with the mineralogical results described above. The development of mixed-layer clay minerals and vermiculite was associated with the oxidation of most of the Fe^{2+} and losses of some interlayer cations. Magnesium also decreased due to the formation of kaolinite and goethite from biotite and to the ejection of some Mg from octahedral sites due to oxidation of Fe^{2+}. Extensive formation of kaolinite and

sesquioxides higher in the profiles resulted in major losses of K, Ca, Na, and Mg. The water content increased markedly with the increasing abundance of hydrous minerals. Aluminum was wholly residual, being present in the secondary minerals gibbsite, kaolinite, and aluminous goethite, and the remaining micaceous minerals. Some Si remained as resistant quartz, but most was present as micaceous minerals and kaolinite.

In each profile the Fe content of altered biotite grains increased. Iron may have been introduced into the porous, exfoliated grains via solution and precipitated as aluminous goethite. Mn and Zn behaved similarly to Mg in that once released from octahedral sites in the remaining micaceous layers, they were removed by leaching. These elements were not retained by the secondary minerals despite the reported association with iron oxides in soils (Mitchell, 1964).

Ni and Cr, however, also present in the octahedral layer of the original mica, exhibited a strongly residual
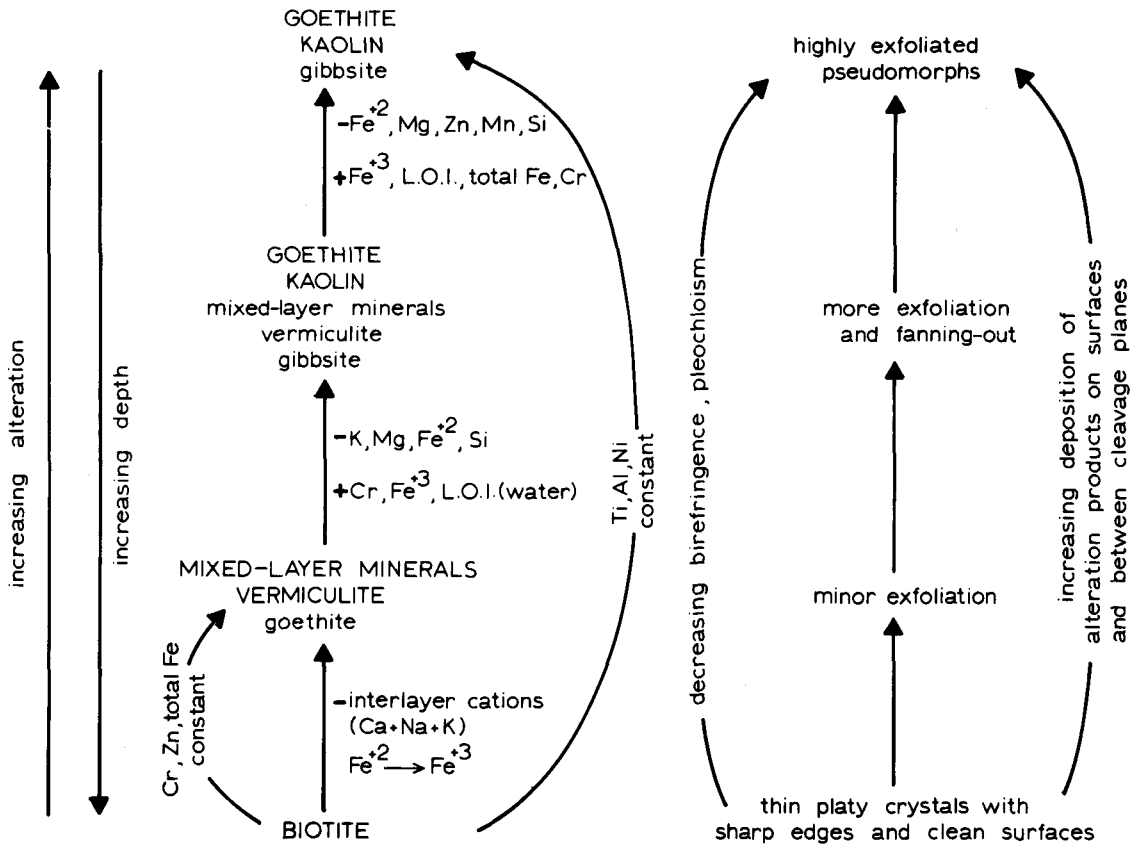
GOETHITE
KAOLIN
gibbsite

$-Fe^{+2}$, Mg, Zn, Mn, Si

$+Fe^{+3}$, L.O.I., total Fe, Cr

GOETHITE
KAOLIN
mixed-layer minerals
vermiculite
gibbsite

$-K$, Mg, Fe^{+2}, Si

$+Cr$, Fe^{+3}, L.O.I. (water)

MIXED–LAYER MINERALS
VERMICULITE
goethite

$-$interlayer cations
(Ca+Na+K)

$Fe^{+2} \longrightarrow Fe^{+3}$

BIOTITE

increasing alteration

increasing depth

Cr, Zn, total Fe constant

Ti, Al, Ni constant

decreasing birefringence, pleochroism

highly exfoliated
pseudomorphs

more exfoliation
and fanning-out

minor exfoliation

thin platy crystals with
sharp edges and clean surfaces

increasing deposition of alteration products on surfaces and between cleavage planes

Figure 14. Pathways for biotite alteration deduced from morphological, mineralogical, and chemical studies of specimens from deeply weathered profiles at Jarrahdale, southwestern Australia. Mineral names in upper case represent major phases; those in lower case represent minor phases.

character in L and R profiles. Neither element is normally found in kaolinite or gibbsite, so both are probably present as structural constituents of goethite. Chromium was also wholly residual in B profile, consistent with its ability to substitute for Fe^{3+} in hematite which comprises a significant proportion of the Fe in altered biotite grains in the upper horizons of this profile. Additional Cr may have been introduced from solution. Substantial losses of Ni occurred which may be a consequence of the incompatibility of Ni with the hematite structure.

The results described above differ in several respects from those published by Kato (1965) for altered biotite grains. He showed that Al increased, Na and Si remained constant, and Fe and Mn decreased in concentration. The Ti concentration also greatly decreased so that all elements would have shown a relative increase if Ti had been used as an immobile reference element. The very large differences in Ti concentration in Kato's specimens as well as his questionable separation procedures and mineralogical data indicate that his specimens may not all have been derived from biotites of the

same initial composition and thus do not represent a true weathering sequence.

Electron microprobe analysis showed that highly altered biotite grains from the upper horizons of the profiles were heterogeneous (Figure 13). Packets or flakes of altered biotite (Fe-, Al-, Mg-, Si-, K-rich) in exfoliated grains were separated by deposits of secondary minerals (Fe-, Al-rich; Mg-, Si-, K-deficient). This distribution is consistent with optical and electron microscopic evidence which showed the presence of infillings and coatings of aluminous goethite, kaolinite, and gibbsite.

The distribution of elements in grains is consistent with the trends in mineralogical and chemical composition of bulk samples of altered biotite grains that were described above. Packets of residual biotite, vermiculite, and mixed-layer clay minerals probably contain most of the Mg, K, Ca, Na, Zn, and Mn in the grains, whereas Fe, Al, Si, Ni, and Cr are present in both these minerals and the secondary minerals. With increasing alteration, the volume of each grain occupied by secondary minerals increased. Although alteration prod-

ucts usually occupy parallel zones between flakes of residual micaceous minerals, altered zones develop that extend perpendicular to flakes (see lower right-hand part of region shown in Figure 13). These regions correspond to the concavities and etchpits in basal surfaces of cleaved grains.

CONCLUSIONS

Biotite weathering is clearly a more complex process than the simple oxidation of iron or changes in the cation-exchange characteristics that occur in laboratory weathering experiments. The relationships between the morphology, mineralogy, and chemistry of weathering biotite grains are depicted in Figure 14.

Within a single biotite grain, oxidation, cation ejection, K-exchange, and development of secondary minerals occur simultaneously resulting in the formation of a mineralogically complex pseudomorph. Discrete vermiculite and vermiculite-dominant mixed-layer minerals are clearly not the normal weathering products in these soils. Packets of a hydrobiotite-like phase develop within a grain and are progressively replaced by kaolinite, goethite, gibbsite, and hematite. The behavior of major and trace elements released from octahedral and interlayer sites during biotite weathering are strongly influenced by the nature of these mineralogical transformations.

ACKNOWLEDGMENT

REFERENCES

Brindley, G. W. and MacEwan, D. M. C. (1953) Structural aspects of the mineralogy of clays: in *Ceramics—a symposium,* British Ceramic Society, Stoke-on-Trent, 15–69.

Eswaran, H. and Bin, W. C. (1978) A study of a deep weathering profile on granite in Peninsular Malaysia: III. Alteration of feldspars: *Soil Sci. Soc. Am. J.* **42,** 154–158.

Eswaran, H. and Heng, Y. Y. (1976) The weathering of biotite in a profile on gneiss in Malaysia: *Geoderma* **16,** 9–20.

Fanning, D. S. and Keramidas, V. Z. (1977) Micas: in *Minerals in Soil Environments,* J. B. Dixon and S. B. Weed, eds., Soil Science Society of America, Madison, Wisconsin, 195–258.

Farmer, V. C., Russell, J. D., McHardy, W. J., Newman, A. C. D., Alhrichs, J. L., and Rimsaite, J. Y. H. (1971) Evidence for loss of protons and octahedral iron from oxidized biotites and vermiculites: *Mineral. Mag.* **38,** 121–137.

Gandolfi, G. (1967) Discussion upon methods to obtain X-ray powder patterns from a single crystal: *Mineral. Petrogr. Acta* **13,** 67–74.

Gilkes, R. J. (1973) The alteration products of potassium-depleted oxybiotite: *Clays & Clay Minerals* **21,** 303–313.

Gilkes, R. J. and Suddhiprakarn, A. (1979) Biotite alteration in deeply weathered granite II. The oriented growth of secondary minerals: *Clays & Clay Minerals* **27,** 361–367.

Gilkes, R. J., Young, R. C., and Quirk, J. P. (1972) The oxidation of octahedral iron in biotite: *Clays & Clay Minerals* **20,** 303–315.

Jackson, M. L., Lee, S. Y., Brown, J. L., Sachs, I. B., and Syers, J. K. (1973) Scanning electron microscopy of hydrous metal oxide crusts intercalated in naturally weathered micaceous vermiculite: *Soil Sci. Soc. Amer. Proc.* **37,** 127–131.

Kato, Y. (1965) Mineralogical study of weathering products of granodiorite at Shinshiro City: Weathering of primary minerals, mineralogical characteristics of weathered mineral grains: *Soil Sci. Plant Nutr. (Tokyo)* **11,** 30–40.

Klug, H. P. and Alexander, L. E. (1974) *X-ray Diffraction Procedures for Polycrystalline and Amorphous Materials*: Wiley, New York, 966 pp.

Leonard, R. A. and Weed, S. B. (1970) Effects of potassium removal on the b-dimension of phlogopite: *Clays & Clay Minerals* **18,** 197–202.

Mitchell, R. L. (1964) Trace elements in soils: in *Chemistry of the Soil,* F. E. Bear, ed., Reinhold, New York, 320–366.

Norrish, K. (1973) Factors in the weathering of mica to vermiculite: *Proc. 1972 Int. Clay Minerals Conf., Madrid,* 417–432.

Norrish, K. and Hutton, J. T. (1969) An accurate X-ray spectrographic method for the analysis of a wide range of geological samples: *Geochim. Cosmochim. Acta* **33,** 431–453.

Norrish, K. and Taylor, R. M. (1961) The ismorphous replacement of iron by aluminium in soil goethite: *J. Soil Sci.* **12,** 294–306.

Radoslovich, E. W. (1963) Cell dimension studies on layer lattice silicates: A summary: *Clays & Clay Minerals* **11,** 225–228.

Radoslovich, E. W. (1975) Micas in macroscopic forms: in *Soil Components: Vol. 2—Inorganic Components,* J. E. Gieseking, ed., Springer Verlag, New York, 27–57.

Reichenbach, H. Graf von and Rich, C. I. (1975) Fine-grained micas in soils: in *Soil Components: Vol. 2—Inorganic Components,* J. E. Gieseking, ed., Springer Verlag, New York, 59–95.

Rhoades, J. D. and Coleman, N. T. (1967) Interstratification in vermiculite and biotite produced by potassium sorption. I. Evaluation by simple X-ray diffraction pattern inspection: *Soil Sci. Soc. Amer. Proc.* **31,** 366–372.

Ruiz-Amil, A., Garcia, A. R., and MacEwan, D. M. C. (1967) *X-ray Diffraction Curves for the Analysis of Interstratified Structures*: Volturna Press, Edinburgh.

Sadleir, S. B. and Gilkes, R. J. (1976) Development of bauxite in relation to parent material near Jarrahdale, Western Australia: *J. Geol. Soc. Aust.* **23,** 333–344.

Sawhney, B. L. (1967) Interstratification in vermiculite: *Clays & Clay Minerals* **15,** 75–84.

Schwertmann, U. and Taylor, R. M. (1977) Iron oxides: in *Minerals in Soil Environments,* J. B. Dixon and S. B. Weed, eds., Soil Science Society of America, Madison, Wisconsin, 145–176.

Suito, E. and Nakahira, M. (1971) Micas and related minerals: in *The Electron-Optical Investigation of Clays,* J. A. Gard, ed., Mineralogical Society, London, 231–255.

Резюме—Биотит в глубоко выветренных гранитных породах в юго-западной Австралии был изменен в расслоенные зерна, состоящие из биотита, смешанно-слойных минералов, каолинита, вермикулита, гиббсита, гетита, и гематита. Дискретный вермикулит и смешанно-слойные глинистые минералы, в основном содержащие вермикулит, не являются основными продуктами выветривания. Окисление октаэдрического железа в биотите ассоциируется с выбросом октаэдрических катионов, потерей межслойного K, и сокращением b-измерения пластин биотита. Si, Mg, Ca, Mn, K, и Na высвобождается из биотита во время выветривания, a Ti, Al, Ni, и Cr остаются. Во время выветривания в зернах появляется добавочная вода и Fe. Много Fe встречается в виде агрегатов микрокристаллических богатых алюминием гетитовых частиц на чешуйчатых поверхностях, меньшие количества встречаются в виде гексагонально расположенных пластинчатых кристаллов гетита на чешуйчатых поверхностях.

Resümee—Der Biotit in den tiefgründig verwitterten, granitischen Gesteinen von Südwest-Australien ist in schuppige Körner umgewandelt, die aus Biotit, Wechsellagerungen, Kaolinit, Vermiculit, Gibbsit, Goethit, und Hämatit bestehen. Einzelne, diskrete Vermiculite und vorwiegend aus Vermiculit bestehende Wechsellagerungen kommen dagegen nicht oft als Verwitterungsprodukte vor. Die Oxidation des oktaedrischen Eisens im Biotit ist mit dem Austritt von oktaedrischen Kationen, dem Verlust von Kalium aus den Zwischenschichten und einer Verkleinerung der Biotitschicht in Richtung der b-Achse verbunden. Während der Verwitterung verarmt der Biotit an Si, Mg, Ca, Mn, K, und Na, während Ti, Al, Ni, und Cr zurückgehalten werden. Fe und Wasser werden den Körnern während der Verwitterung zugeführt. Ein großer Teil des Fe ist in Form von Aggregaten aus mikrokristallinen, aluminiumreichen Goethitpartikeln auf den Blättchenoberflächen und in Ätzgruben vorhanden. Ein kleiner Teil kommt in Form von hexagonalen Anordnungen aus leistenförmigen Goethitkristallen auf den Blättchenoberflächen vor.

Résumé—La biotite dans des roches granitiques profondément altérées d'Australie du Sud-ouest a été altérée en grains exfoliés composés de biotite, de minéraux argileux à couches mélangées, de kaolinite, de vermiculite, de gibbsite, de goethite, et d'hématite. La vermiculite elle-même, et les minéraux argileux à couches mélangées à prédominance de vermiculite ne sont pas des produits d'altération majeurs. L'oxidation de fer octaédrique dans la biotite est associée avec l'éjection de cations octaédriques, avec la perte de l'intercouche K, et avec la contraction de la dimension-b de la feuille de biotite. Si, Mg, Ca, Mn, K, et Na sont perdus par la biotite pendant l'altération, et Ti, Al, Ni, and Cr sont retenus. Fe et de l'eau ont été ajoutés aux grains pendant l'altération. Beaucoup de Fe existe comme aggrégats de particules de goethite microcristallins et riches en aluminium sur des surfaces de lame et dans des crevasses gravées, avec des quantités moindres existant comme arrangements hexagonaux de cristaux de goethite en forme de latte sur les surfaces des lames.